

Supplementary Information for:

**Spin State Solvomorphism in a Series of Rare S = 1
Manganese(III) Complexes**

Andrew Barker,^{a†} Conor T. Kelly,^{a†} Irina A. Kühne,^a Stephen Hill,^{b,c} J. Krzystek,^b Paul Wix,^d Kane Esien,^e Solveig Felton,^e Helge Müller-Bunz^a and Grace G. Morgan^{*a}

Email: grace.morgan@ucd.ie

- a. School of Chemistry, University College Dublin (UCD), Belfield, Dublin 4, Ireland.
- b. National High Magnetic Field Laboratory, Florida State University, Tallahassee, FL 32310, USA.
- c. Department of Physics, Florida State University, Tallahassee, FL 32306, USA.
- d. School of Chemistry & CRANN Institute, Trinity College Dublin, University of Dublin, College Green, Dublin 2, Ireland.
- e. Centre for Nanostructured Media (CNM), School of Mathematics and Physics, Queen's University Belfast, Belfast, BT7 1NN, UK.

[†]These authors contributed equally to the work.

Contents

S.1 Magnetic Susceptibility Data.....	2
S.2 High Field Electron Paramagnetic Resonance (HFEPR)	7
S.3 Single Crystal X-Ray Diffraction of 1, 2, 2·0.5EtOH, 3·0.5EtOH, 4	8
S.4 X-Ray Crystal Structure of 2, 2·0.5EtOH, 3·0.5EtOH, 4	9
S.5 Crystallographic Data for 1, 2, 2·0.5EtOH, 3·0.5EtOH and 4.....	11
S.6 Distortion Parameters for 1, 2, 2·0.5EtOH, 3·0.5EtOH, 4.....	15
S.7 Intermolecular Interactions of 1, 2, 2·0.5EtOH, 3·0.5EtOH, 4	16
S.8 Infrared Spectra of 1, 2, 2·0.5EtOH, 3, 3·0.5EtOH and 4.....	19
S.9 UV-Visible Spectra of 1 – 4, 2·0.5EtOH and 3·0.5EtOH	20
S.10 Powder X-Ray Diffraction	22

S.1 Magnetic Susceptibility Data

Table S.1 Magnetic susceptibility data for complexes **1 – 4**, **2·0.5EtOH** and **3·0.5EtOH** from 2 K to 300 K.

[Mn(napsal ₂ 323)]NTf ₂ (1)		[Mn(napsal ₂ 323)]ClO ₄ (2)		[Mn(napsal ₂ 323)]BF ₄ (3)	
T (K)	$\chi_M T$ (cm ³ K mol ⁻¹)	T (K)	$\chi_M T$ (cm ³ K mol ⁻¹)	T (K)	$\chi_M T$ (cm ³ K mol ⁻¹)
300.05	1.1447	300.06	1.4025	5.0134	0.3783
290.19	1.1172	290.2	1.379	10	0.66918
279.83	1.0942	279.82	1.3566	15.01	0.82765
269.81	1.0759	269.85	1.335	19.999	0.90646
259.8	1.062	259.8	1.3128	25.001	0.9492
249.78	1.0506	249.78	1.2904	29.999	0.97332
239.74	1.0424	239.75	1.2676	35	0.98921
229.75	1.0366	229.74	1.2456	40	1.0028
219.73	1.0317	219.74	1.2227	45	1.0102
209.74	1.029	209.74	1.2	50.011	1.0169
199.74	1.0269	199.75	1.178	55.025	1.0225
189.74	1.0254	189.79	1.1568	60.038	1.0266
179.75	1.0253	179.77	1.1343	65.056	1.0298
169.78	1.0244	169.77	1.1129	70.064	1.0327
159.83	1.0244	159.83	1.0916	75.074	1.0354
149.9	1.0244	149.88	1.0731	80.085	1.0377
139.95	1.0247	139.96	1.057	85.097	1.0398
130	1.025	130	1.0435	90.121	1.042
120.04	1.025	120.04	1.0326	95.128	1.0435
110.08	1.0276	110.07	1.0246	100.11	1.045
100.06	1.0248	100.06	1.0167	105.13	1.0468
94.987	1.024	94.968	1.0141	110.16	1.0488
90.052	1.0231	90.049	1.0116	115.16	1.0501
85.066	1.0226	85.061	1.0103	120.19	1.0517
80.051	1.0211	80.04	1.0073	125.18	1.0534
75.05	1.0196	75.051	1.005	130.21	1.0549
70.048	1.0175	70.045	1.0027	135.2	1.0558
65.042	1.0152	65.039	1.0009	140.19	1.0572
60.071	1.0131	60.078	0.99886	145.23	1.0583
55.06	1.01	55.061	0.9961	150.27	1.0602

50.043	1.0056	50.038	0.99257	155.22	1.061
45.022	1.0001	45.019	0.98785	160.25	1.0622
40.002	0.99286	40.004	0.98188	165.25	1.0632
34.997	0.98303	34.997	0.97396	170.27	1.0653
29.995	0.9688	29.993	0.96194	175.27	1.0662
27.998	0.96093	27.992	0.95687	180.28	1.0682
26.004	0.95173	26.002	0.94963	185.3	1.0698
24.003	0.94046	23.999	0.94065	190.3	1.0716
22.002	0.92613	21.999	0.92948	195.31	1.0728
20.004	0.90801	20	0.91646	200.31	1.0741
18.003	0.88505	18.001	0.89846	205.32	1.0758
16.005	0.8552	16.002	0.87343	210.33	1.0783
14.011	0.81581	14.007	0.83651	215.32	1.0802
12.008	0.76138	12.009	0.78367	220.32	1.0821
11.015	0.72975	11.013	0.7533	225.33	1.0848
10.503	0.71088	10.495	0.73697	230.31	1.0874
9.9877	0.69057	9.979	0.71737	235.34	1.0903
9.4728	0.66903	9.4684	0.69569	240.34	1.0931
8.9646	0.64599	8.9611	0.67217	245.33	1.0963
8.4517	0.62142	8.4493	0.64556	250.34	1.1007
7.9418	0.59516	7.9356	0.61627	255.35	1.1049
7.4284	0.56693	7.4234	0.58498	260.34	1.11
6.9167	0.53714	6.9116	0.55237	265.35	1.1142
6.4068	0.5062	6.4013	0.51793	270.35	1.1206
5.8959	0.47379	5.8935	0.48265	275.33	1.1271
5.3833	0.44029	5.3801	0.44578	280.33	1.1341
4.8713	0.4058	4.8678	0.40813	285.33	1.1416
4.3533	0.37024	4.3491	0.36982	290.32	1.1493
3.8467	0.33501	3.8443	0.33108	295.34	1.1583
3.3344	0.29832	3.3344	0.2922	300.35	1.1694
2.8246	0.2618	2.8217	0.2518		
2.3152	0.22487	2.3119	0.21084		
1.8015	0.18649	1.7983	0.16804		

[Mn(napsal ₂ 323)]NO ₃ (4)		[Mn(napsal ₂ 323)]ClO ₄ ·0.5EtOH (2·0.5EtOH)		[Mn(napsal ₂ 323)]BF ₄ ·0.5EtOH (3·0.5EtOH)	
T (K)	$\chi_{\text{M}}T$ (cm ³ K mol ⁻¹)	T (K)	$\chi_{\text{M}}T$ (cm ³ K mol ⁻¹)	T (K)	$\chi_{\text{M}}T$ (cm ³ K mol ⁻¹)
300.05	1.1856	300.07	2.8421	300.06	3.0959
294.22	1.1705	290.21	2.8397	290.22	3.0847
287.49	1.1553	279.82	2.845	279.91	3.0836
281.55	1.143	269.81	2.8472	269.92	3.0793
275.55	1.1317	259.76	2.849	259.89	3.0766
269.53	1.1215	249.77	2.8524	249.88	3.0727
263.45	1.112	239.74	2.852	239.83	3.0699
257.46	1.1043	229.74	2.8534	229.78	3.0661
251.47	1.0978	219.73	2.8546	219.77	3.061
245.46	1.0914	209.74	2.8583	209.75	3.056
239.42	1.0859	199.73	2.8583	199.75	3.0489
233.42	1.0811	189.73	2.8641	189.75	3.0433
227.42	1.0775	179.76	2.8702	179.74	3.0362
221.39	1.074	169.77	2.8737	169.77	3.0287
215.39	1.0707	159.93	2.8781	159.81	3.0193
209.36	1.0681	149.98	2.8841	149.86	3.0101
203.35	1.0655	139.95	2.8822	139.93	3.0013
197.33	1.0638	130.01	2.8882	129.99	2.9937
191.31	1.062	120.04	2.8944	120.03	2.9833
185.29	1.0612	110.07	2.8996	110.07	2.9696
179.28	1.0602	100.04	2.9021	100.05	2.946
173.26	1.0593	94.983	2.9089	94.966	2.9376
167.27	1.0583	90.051	2.9152	90.07	2.9272
161.26	1.0572	85.052	2.92	85.063	2.9169
155.22	1.0563	80.046	2.9256	80.047	2.9051
149.21	1.0557	75.053	2.9305	75.052	2.8973
143.2	1.0553	70.041	2.9398	70.043	2.8821
137.18	1.0551	65.044	2.9507	65.043	2.8681
131.19	1.0551	60.033	2.9593	60.068	2.8474
125.19	1.0555	55.057	2.9706	55.061	2.8295
119.22	1.0557	50.043	2.9839	50.043	2.8131
113.26	1.0555	45.018	2.9991	45.028	2.8038
107.3	1.0554	40.004	3.015	40.007	2.7906
101.39	1.0532	34.997	3.031	34.996	2.7808

95.377	1.0527	29.995	3.0556	29.995	2.7797
89.421	1.0529	28.003	3.0695	27.994	2.7837
83.39	1.0521	26.002	3.0865	26.003	2.7843
77.366	1.0502	23.997	3.1066	23.999	2.788
71.342	1.0486	21.998	3.126	21.999	2.7896
65.289	1.0463	20	3.1475	20.001	2.792
59.25	1.0437	18.001	3.161	18.001	2.7926
53.213	1.0401	16.001	3.1661	16.002	2.7865
47.157	1.0358	14.007	3.1702	14.007	2.7755
41.124	1.0298	12.004	3.1482	12.006	2.7476
35.103	1.0209	11.009	3.1452	11.009	2.7366
29.074	1.0067	10.492	3.1394	10.496	2.7296
23.058	0.98016	9.9806	3.1315	9.9806	2.7216
17.042	0.92254	9.4682	3.1248	9.4687	2.7099
11.039	0.7728	8.958	3.115	8.9574	2.6985
5.0054	0.40603	8.4477	3.0998	8.445	2.6802
		7.9354	3.0789	7.9363	2.6582
		7.4248	3.0547	7.4244	2.6302
		6.9135	3.0173	6.9146	2.5874
		6.4024	2.9734	6.4026	2.5438
		5.8919	2.9194	5.8929	2.4816
		5.3789	2.8565	5.3803	2.3898
		4.8674	2.7703	4.8684	2.2582
		4.3479	2.662	4.3494	2.1035
		3.844	2.5232	3.8454	1.9114
		3.3328	2.3355	3.3344	1.7276
		2.8221	2.0831	2.8232	1.5279
		2.3122	1.7763	2.3119	1.3081
		1.803	1.4249	1.7953	1.0395

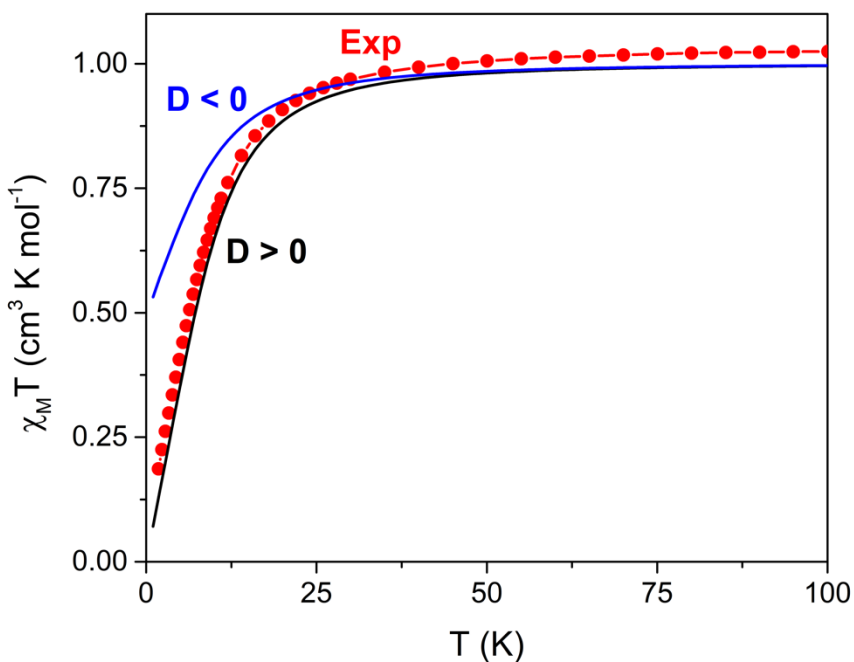


Figure S.1 DC magnetic susceptibility of a polycrystalline sample of **1**, measured in a 1,000 Oe external field. Experimental points are shown in *red* and simulations using a spin Hamiltonian with the parameters recorded in the HFEPR, $|D| = 19.6 \text{ cm}^{-1}$ and $|E| = 2.02 \text{ cm}^{-1}$. The *black* line indicates a positive D value and the *blue* line indicates a negative D value. Simulation was performed using the EasySpin software package.¹

S.2 High Field Electron Paramagnetic Resonance (HFEPR)

HFEPR spectra were recorded at the National High Magnetic Field Laboratory (NHMFL, Tallahassee, FL) using the homodyne transmission spectrometer equipped with a 15/17 T superconducting magnet.² Measurements were carried out on a powder sample of **1** (~30 mg) ground up with eicosane wax. The sample was packed into a Teflon sample holder. Spectra were recorded at 4.5 K and 10 K at multiple frequencies from 203 to 634 GHz in a 0 to 14.5 T field range and the spectrum at 10 K and 203.2 GHz is given in Figure S.2. The 2D magnetic field versus frequency simulations in Figure 3 and the spectral simulations in Figures 2 and S.2, were generated using the following spin $S = 1$ Hamiltonian: $\hat{H} = D\hat{S}_z^2 + E(\hat{S}_x^2 - \hat{S}_y^2) + g\mu_B\vec{B}\cdot\hat{S}$, where the first two terms represent the 2nd order axial and rhombic zero field splitting interactions, parameterized respectively by D and E , and the final term represents the Zeeman interaction: \hat{S} is the spin operator and \hat{S}_i ($i = x, y, z$) its components, \vec{B} is the applied magnetic field vector, \vec{g} the Lande g -factor (assumed to be direction independent for this analysis), and μ_B the Bohr magneton.

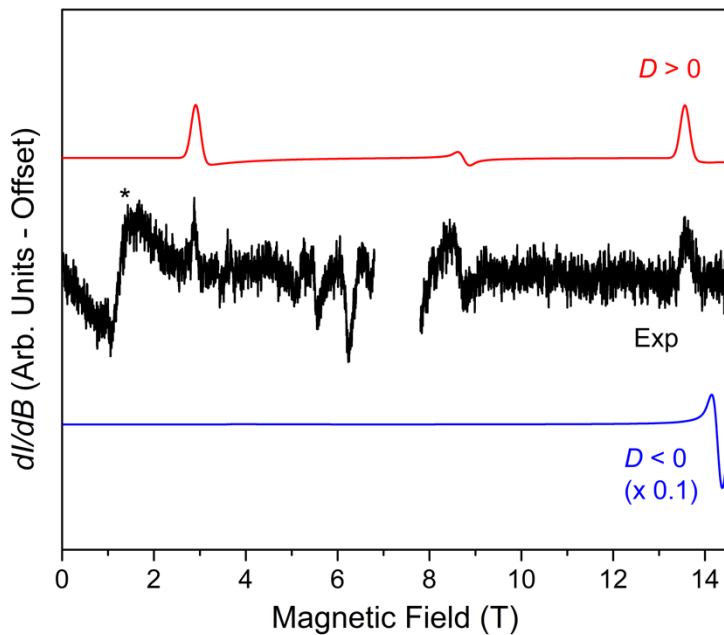


Figure S.2 HFEPR spectrum of **1** recorded at 10 K and 203.2 GHz (black trace). The high-amplitude signal from a Mn(II) impurity at $g = 2.00$ has been removed from the experimental spectrum for clarity. The resonance at 1.35 T (*) cannot be attributed to the $S = 1$ state and its origin remains unknown. The signal at 6.25 T originates from the probe. The two coloured traces are simulations assuming a powder distribution of the microcrystallites, using spin Hamiltonian parameters as in the text, but different sign of D . Red trace represents positive D ; blue trace – negative D . By comparing the experiment with simulations we can unequivocally determine the sign of D as positive.

S.3 Single Crystal X-Ray Diffraction of **1**, **2**, **2·0.5EtOH**, **3·0.5EtOH**, **4**

Single crystal X-ray diffraction was carried out on suitable single crystals using an Oxford Supernova diffractometer (Oxford Instruments, Oxford, United Kingdom). Datasets were measured using monochromatic Cu-K α radiation for **1**, **2**, **4** and **3·0.5EtOH** and monochromatic Mo-K α radiation for **2·0.5EtOH** and corrected for absorption. The temperature was controlled with an Oxford Cryosystem instrument. A complete dataset was collected, assuming that the Friedel pairs are not equivalent. Analytical absorption correction based on the shape of the crystals was performed.³ All structures were solved by dual-space methods (SHELXT)³ and refined by full matrix least-squares on F² for all data using SHELXL-2016.⁴ The hydrogen atoms attached to nitrogen were located in the difference Fourier map and allowed to refine freely. All other hydrogen atoms were added at calculated positions and refined using a riding model. Their isotropic displacement parameters were fixed to 1.2 times the equivalent one of the parent atom. Anisotropic displacement parameters were used for all non-hydrogen atoms. Crystallographic details for all compounds are summarised in Table S.2. Crystallographic data for the structures reported in this paper have been deposited with the Cambridge Crystallographic Data Centre as supplementary publication numbers CCDC-1921981 (**1**, 100 K), CCDC-1921978 (**2**, 100 K), CCDC-1921977 (**2·0.5EtOH**, 100 K), CCDC-1921979 (**3·0.5EtOH**, 100 K), CCDC-1921980 (**4**, 100 K).

S.4 X-Ray Crystal Structure of 2, 2·0.5EtOH, 3·0.5EtOH, 4

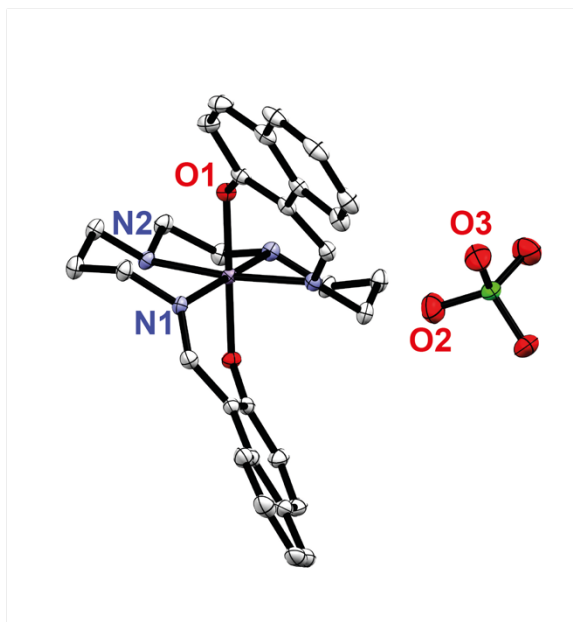


Figure S.3 Structure of **2** recorded at 100 K. Thermal ellipsoids are drawn at 50 % atomic probability. Hydrogen atoms have been omitted for clarity.

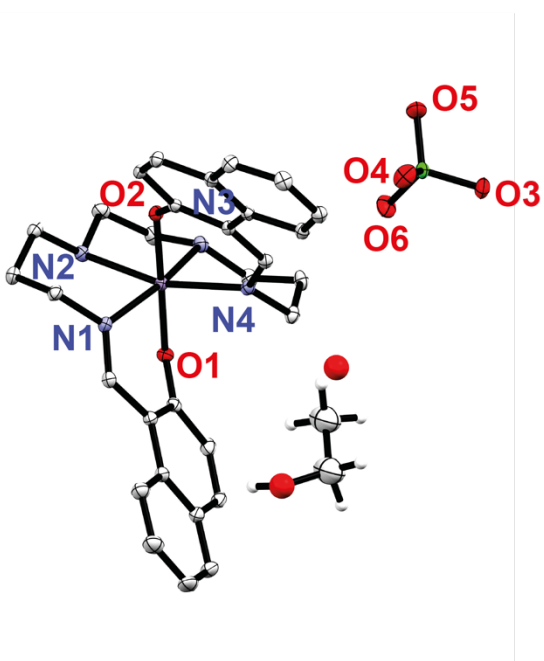


Figure S.4 Structure of **2·0.5EtOH** recorded at 100 K. Thermal ellipsoids are drawn at 50% atomic probability. Hydrogen atoms have been omitted for clarity, except for those on the solvent molecule.

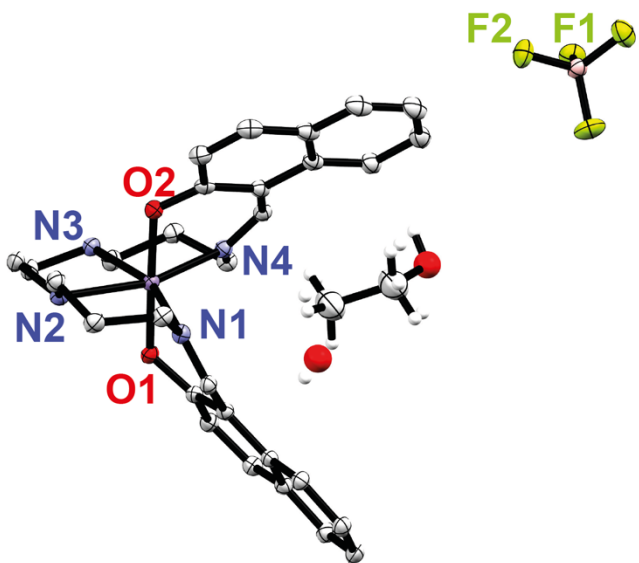


Figure S.5 Structure of **3·0.5EtOH** recorded at 100 K. Thermal ellipsoids are drawn at 50% atomic probability. Hydrogen atoms have been omitted for clarity, except for those on the solvent molecule.

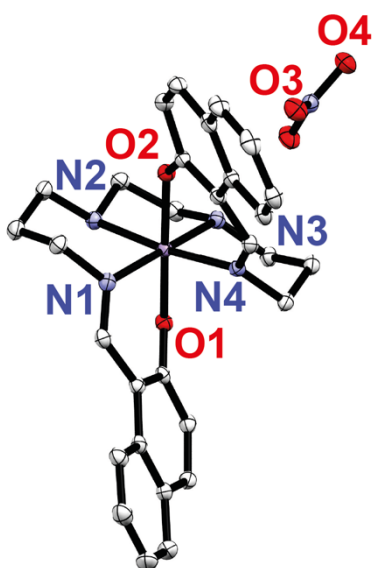


Figure S.6 Structure of **4** recorded at 100 K. Thermal ellipsoids are drawn at 50% atomic probability. Hydrogen atoms have been omitted for clarity, except for those on the solvent molecule.

S.5 Crystallographic Data for 1, 2, 2·0.5EtOH, 3·0.5EtOH and 4

Table S.2 Crystallographic details for complexes 1, 2, 2·0.5EtOH, 3·0.5EtOH and 4.

Compound	[Mn(napsal ₂ 323)]NTf ₂ (1)	[Mn(napsal ₂ 323)]ClO ₄ (2)	[Mn(napsal ₂ 323)]ClO ₄ ·0.5EtOH (2·0.5EtOH)
Empirical Formula	C ₃₂ H ₃₂ N ₅ O ₆ F ₆ S ₂ Mn	C ₃₀ H ₃₂ N ₄ O ₆ ClMn	C ₆₂ H ₇₀ N ₈ O ₁₃ Cl ₂ Mn ₂
Formula Weight	815.68	634.98	1316.04
Crystal System	Triclinic	Orthorhombic	Triclinic
Space Group	P-1 (#2)	P2 ₁ 2 ₁ 2 (#18)	P-1 (#2)
Crystal Size (mm)	0.304 × 0.088 × 0.032	0.231 × 0.117 × 0.077	0.217 × 0.196 × 0.194
a (Å)	8.2729(3)	7.49091(6)	8.2079(1)
b (Å)	15.2825(6)	12.7773(1)	11.8247(2)
c (Å)	15.4726(6)	14.7289(1)	15.7728(2)
α (°)	113.759(4)	90	90.977(1)
β (°)	95.344(3)	90	96.600(1)
γ (°)	99.235(3)	90	106.418(2)
Volume (Å ³)	1740.04(13)	1409.756(18)	1456.71(4)
Z	2	2	1
ρ _{calc} (mg m ⁻³)	1.557	1.496	1.500
T (K)	100(2)	100(2)	100(2)
μ (mm ⁻¹)	4.956	5.118	0.599
F(000)	836	660	686
Limiting Indicies	h = ±10, k = ±19, l = ±19	h = ±6, k = ±16, l = ±18	h = ±11, k = ±16, l = ±22
Reflections			
Collected/ Unique R(int)	12585 / 7246	14804 / 2966	23566 / 8887
Completeness to θ (%)	100.0	99.9	99.8
Data/ Restraints/ Parameters	12585 / 0 / 470	2966 / 0 / 191	8887 / 0 / 401
GooF on F ²	1.148	1.076	1.051
Final R Indices (I>2σ(I))	R ₁ = 0.0437, wR ₂ = 0.1432	R ₁ = 0.0230, wR ₂ = 0.0600	R ₁ = 0.0365, wR ₂ = 0.0834
R Indices (All Data)	R ₁ = 0.0487, wR ₂ = 0.1520	R ₁ = 0.0242, wR ₂ = 0.0610	R ₁ = 0.0492, wR ₂ = 0.0910
Largest Diff. Peak/ Hole (e Å ⁻³)	0.641 and -0.632	0.220 and -0.432	0.467 and -0.421
CCDC Number	1921981	1921978	1921977

Compound	[Mn(napsal ₂ 323)]BF ₄ ·0.5EtOH (3·0.5EtOH)	[Mn(napsal ₂ 323)]NO ₃ (4)
Empirical Formula	C ₆₂ H ₇₀ B ₂ N ₈ O ₅ F ₈ Mn ₂	C ₃₀ H ₃₂ N ₅ O ₅ Mn
Formula Weight	1290.76	597.54
Crystal System	Triclinic	Monoclinic
Space Group	P-1 (#2)	P2 ₁ /c (#14)
Crystal Size (mm)	0.161 × 0.144 × 0.043	0.394 × 0.095 × 0.056
a (Å)	8.1860(1)	7.89419(4)
b (Å)	11.7372(2)	24.6143(1)
c (Å)	15.7620(2)	14.02753(6)
α (°)	90.9985(9)	90
β (°)	96.455(1)	92.2530(4)
γ (°)	106.150(1)	90
Volume (Å ³)	1443.56(4)	2723.58(2)
Z	1	4
d _{calc} (mg m ⁻³)	1.485	1.457
T (K)	100(2)	100(2)
μ (mm ⁻¹)	4.280	4.362
F(000)	670	1248
Limiting Indicies	h = ±10, k = ±14, l = ±19	h = ±9, k = ±31, l = ±17
Reflections Collected/ Unique R(int)	29061 / 5999	56051 / 5715
Completeness to θ (%)	99.3	100.0
Data/ Restraints/ Parameters	5999 / 0 / 401	5715 / 0 / 370
GooF on F ²	1.061	1.081
Final R Indices (I>2σ(I))	R ₁ = 0.0299, wR ₂ = 0.0790	R ₁ = 0.0261, wR ₂ = 0.0724
R Indices (All Data)	R ₁ = 0.0320, wR ₂ = 0.0805	R ₁ = 0.0272, wR ₂ = 0.0734
Largest Diff. Peak/ Hole (e Å ⁻³)	0.337 and -0.407	0.230 and -0.384
CCDC Number	1921979	1921980

Table S.3 Selected bond lengths (\AA) and angles ($^\circ$) for **1**, **2** and **2·0.5EtOH**.

[Mn(napsal ₂ 323)]NTf ₂ (1)		[Mn(napsal ₂ 323)]ClO ₄ (2) [‡]		[Mn(napsal ₂ 323)]ClO ₄ ·0.5EtOH (2·0.5EtOH)	
Bond Length (\AA)					
Mn–O(2)	1.870(2)	Mn–O(1)#1	1.8855(14)	Mn–O(2)	1.8635(10)
Mn–O(1)	1.8753(19)	Mn–O(1)	1.8855(14)	Mn–O(1)	1.8679(10)
Mn–N(1)	1.975(2)	Mn–N(1)	1.9946(17)	Mn–N(1)	2.0846(12)
Mn–N(4)	1.978(2)	Mn–N(1)#1	1.9946(17)	Mn–N(4)	2.1143(13)
Mn–N(3)	2.058(2)	Mn–N(2)	2.0630(17)	Mn–N(2)	2.2381(13)
Mn–N(2)	2.063(2)	Mn–N(2)#1	2.0630(17)	Mn–N(3)	2.2429(13)
Bond Angles ($^\circ$)					
O(2)–Mn–O(1)	173.68(8)	O(1)#1–Mn–O(1)	179.49(9)	O(2)–Mn–O(1)	178.68(5)
O(2)–Mn–N(1)	94.85(9)	O(1)#1–Mn–N(1)	92.68(7)	O(2)–Mn–N(1)	92.41(5)
O(1)–Mn–N(1)	89.17(9)	O(1)–Mn–N(1)	87.65(7)	O(1)–Mn–N(1)	86.29(5)
O(2)–Mn–N(4)	88.91(9)	O(1)#1–Mn–N(1)#1	87.65(7)	O(2)–Mn–N(4)	86.52(5)
O(1)–Mn–N(4)	95.45(9)	O(1)–Mn–N(1)#1	92.68(7)	O(1)–Mn–N(4)	93.73(5)
N(1)–Mn–N(4)	97.12(9)	N(1)–Mn–N(1)#1	96.97(9)	N(1)–Mn–N(4)	111.15(5)
O(2)–Mn–N(3)	89.66(9)	O(1)#1–Mn–N(2)	87.98(7)	O(2)–Mn–N(2)	85.56(5)
O(1)–Mn–N(3)	85.87(9)	O(1)–Mn–N(2)	91.64(7)	O(1)–Mn–N(2)	94.60(5)
N(1)–Mn–N(3)	172.58(9)	N(1)–Mn–N(2)	89.52(7)	N(1)–Mn–N(2)	86.79(5)
N(4)–Mn–N(3)	88.84(9)	N(1)#1–Mn–N(2)	172.34(7)	N(4)–Mn–N(2)	160.67(5)
O(2)–Mn–N(2)	85.58(9)	O(1)#1–Mn–N(2)#1	91.64(7)	O(2)–Mn–N(3)	94.54(5)
O(1)–Mn–N(2)	89.62(9)	O(1)–Mn–N(2)#1	87.98(7)	O(1)–Mn–N(3)	86.78(5)
N(1)–Mn–N(2)	88.98(9)	N(1)–Mn–N(2)#1	172.34(7)	N(1)–Mn–N(3)	163.63(5)
N(4)–Mn–N(2)	172.11(9)	N(1)#1–Mn–N(2)#1	89.52(7)	N(4)–Mn–N(3)	84.09(5)
N(3)–Mn–N(2)	85.49(9)	N(2)–Mn–N(2)#1	84.31(10)	N(2)–Mn–N(3)	79.00(5)

[‡] Symmetry transformations used to generate equivalent atoms: #1 $-x, -y+1, z$; #2 $-x+1, -y+1, z$

Table S.4 Selected bond lengths (\AA) and angles ($^\circ$) for **3·0.5EtOH** and **4**.

[Mn(napsal ₂ 323)]BF ₄ ·0.5EtOH (3·0.5EtOH)	[Mn(napsal ₂ 323)]NO ₃ (4)		
Bond Length (Å)			
Mn–O(1)	1.8671(10)	Mn–O(1)	1.8762(8)
Mn–O(2)	1.8701(10)	Mn–O(2)	1.8803(8)
Mn–N(4)	2.0872(12)	Mn–N(4)	1.9825(10)
Mn–N(1)	2.1211(11)	Mn–N(1)	1.9876(11)
Mn–N(2)	2.2398(12)	Mn–N(2)	2.0548(10)
Mn–N(3)	2.2426(11)	Mn–N(3)	2.0573(10)
Bond Angles (°)			
O(1)–Mn–O(2)	178.77(4)	O(1)–Mn–O(2)	175.44(3)
O(1)–Mn–N(4)	92.50(4)	O(1)–Mn–N(4)	93.54(4)
O(2)–Mn–N(4)	86.32(4)	O(2)–Mn–N(4)	88.36(4)
O(1)–Mn–N(1)	86.48(4)	O(1)–Mn–N(1)	88.51(4)
O(2)–Mn–N(1)	93.62(4)	O(2)–Mn–N(1)	95.42(4)
N(4)–Mn–N(1)	111.20(4)	N(4)–Mn–N(1)	95.91(4)
O(1)–Mn–N(2)	94.24(4)	O(1)–Mn–N(2)	90.68(4)
O(2)–Mn–N(2)	86.99(4)	O(2)–Mn–N(2)	87.07(4)
N(4)–Mn–N(2)	163.73(4)	N(4)–Mn–N(2)	173.45(4)
N(1)–Mn–N(2)	84.01(4)	N(1)–Mn–N(2)	89.20(4)
O(1)–Mn–N(3)	85.49(4)	O(1)–Mn–N(3)	86.16(4)
O(2)–Mn–N(3)	94.79(4)	O(2)–Mn–N(3)	89.70(4)
N(4)–Mn–N(3)	86.82(4)	N(4)–Mn–N(3)	90.01(4)
N(1)–Mn–N(3)	160.57(4)	N(1)–Mn–N(3)	172.28(4)
N(2)–Mn–N(3)	78.98(4)	N(2)–Mn–N(3)	85.28(4)

S.6 Distortion Parameters for 1, 2, 2·0.5EtOH, 3·0.5EtOH, 4

Octahedral distortion parameters were determined with the use of: *OctaDist* - A program for determining the structural distortion of the octahedral complexes. (<https://octadist.github.io>)

The distortion parameter Θ is a measure of the deviation of the metal centre geometry from perfect octahedron (O_h) to trigonal prismatic (D_{3h}). It is calculated by the sum of the deviation of the 24 unique ligand-metal-ligand angles (θ) from 60° as per Equation S.1:

$$\Theta = \sum_{i=1}^{24} |60 - \theta_i|$$

The more distorted the octahedron the higher the Θ value, therefore as the HS state is expected to be more distorted, a higher the value of Θ should be observed in the HS state, and consequently a lower value of Θ in the LS state.⁵

The distortion parameter Σ is a measure of the sum of the deviation from 90° of the 12 cis angles (ϕ) in the metal coordination sphere, given by Equation S.2:

$$\Sigma = \sum_{i=1}^{12} |90 - \phi_i|$$

Similarly, the HS state is expected to be more distorted so the value of Σ should be greater for the HS state.

Table S.5 Distortion parameters Σ and Θ for 1, 2, 2·0.5EtOH, 3·0.5EtOH, 4.

Complex	1	2	2·0.5EtOH	3·0.5EtOH	4
Σ (°)	35.32	30.97	71.37	71.25	31.27
Θ (°)	97.20	97.07	238.81	239.22	88.41

The distortion parameters correspond with the expected ranges of literature values for the complexes in the IS and HS state respectively, with the IS ($S = 1$) state expected to have a value of $\Sigma = 30^\circ - 50^\circ$ and $\Theta = 80^\circ - 100^\circ$ and the HS ($S = 2$) state expected to have a value of $\Sigma = 60^\circ - 70^\circ$ and $\Theta = 140^\circ - 220^\circ$.⁶

S.7 Intermolecular Interactions of 1, 2, 2·0.5EtOH, 3·0.5EtOH, 4

Table S.6 Hydrogen bonds for complexes **1**, **2**, **2·0.5EtOH**, **3·0.5EtOH**, **4**.

Complex	D–H...A	d(D–H) (Å)	d(H...A) (Å)	d(D...A) (Å)	<(DHA) (°)
1[†]	N(2)–H(1N2)...O(3)#1	1.00	2.32	3.134(3)	138.0
	N(3)–H(1N3)...O(6)	1.00	2.27	3.141(3)	145.0
2[‡]	N(2)–H(1N2)...O(2)#1	1.00	2.41	3.054(2)	121.9
2·0.5EtOH^x	N(2)–H(1N2)...O(3)#1	1.00	2.36	3.212(2)	143.0
3·0.5EtOH[*]	N(3)–H(1N3)...F(1)#1	1.00	2.30	3.150(2)	142.1
4[†]	N(2)–H(2A)...O(3)#1	0.98	2.22	3.155(3)	159.6
	N(3)–H(3A)...O(3)	0.98	2.21	3.078(3)	147.4

[†]Symmetry transformations used to generate equivalent atoms: #1 x-1,y,z

[‡]Symmetry transformations used to generate equivalent atoms: #1 -x+1,-y+1,-z+1

*Symmetry transformations used to generate equivalent atoms: #1 x,y-1,z

*Symmetry transformations used to generate equivalent atoms: #1 -x+1,-y,-z+1

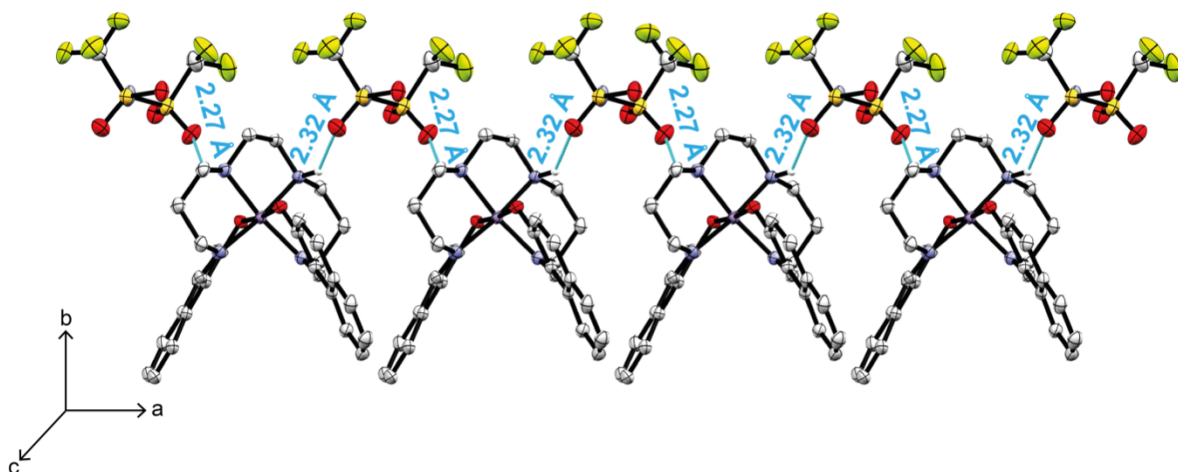


Figure S.7 1-D Hydrogen bonding network in **1** with ellipsoids drawn at 50% atomic probability. Hydrogen atoms, except those involved in the hydrogen bonding, have been omitted for clarity.

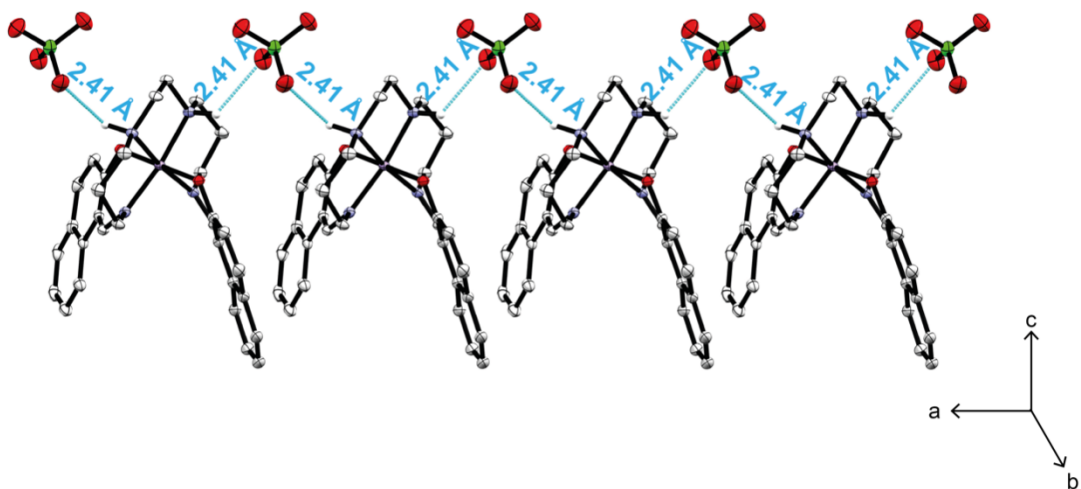


Figure S.8 1-D Hydrogen bonding network in **2** with ellipsoids drawn at 50% atomic probability. Hydrogen atoms, except those involved in the hydrogen bonding, have been omitted for clarity.

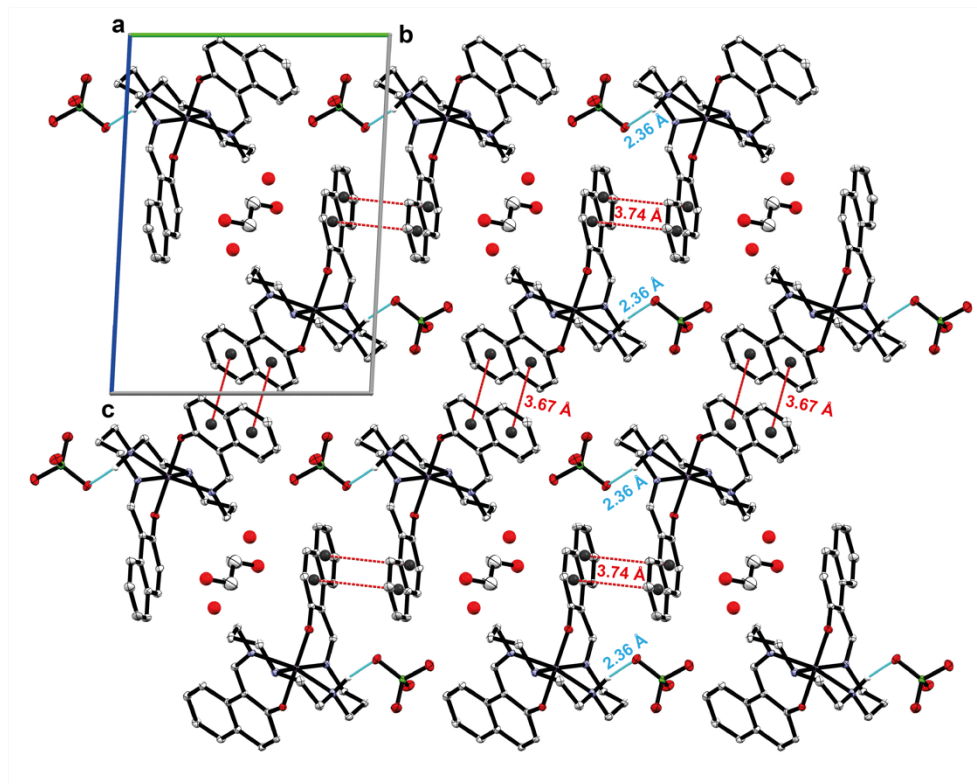


Figure S.9 Hydrogen bonding (**blue**) and π - π stacking (**red**) interactions in **2·0.5EtOH** with ellipsoids drawn at 50% atomic probability. Hydrogen atoms, except those involved in the hydrogen bonding, have been omitted for clarity.

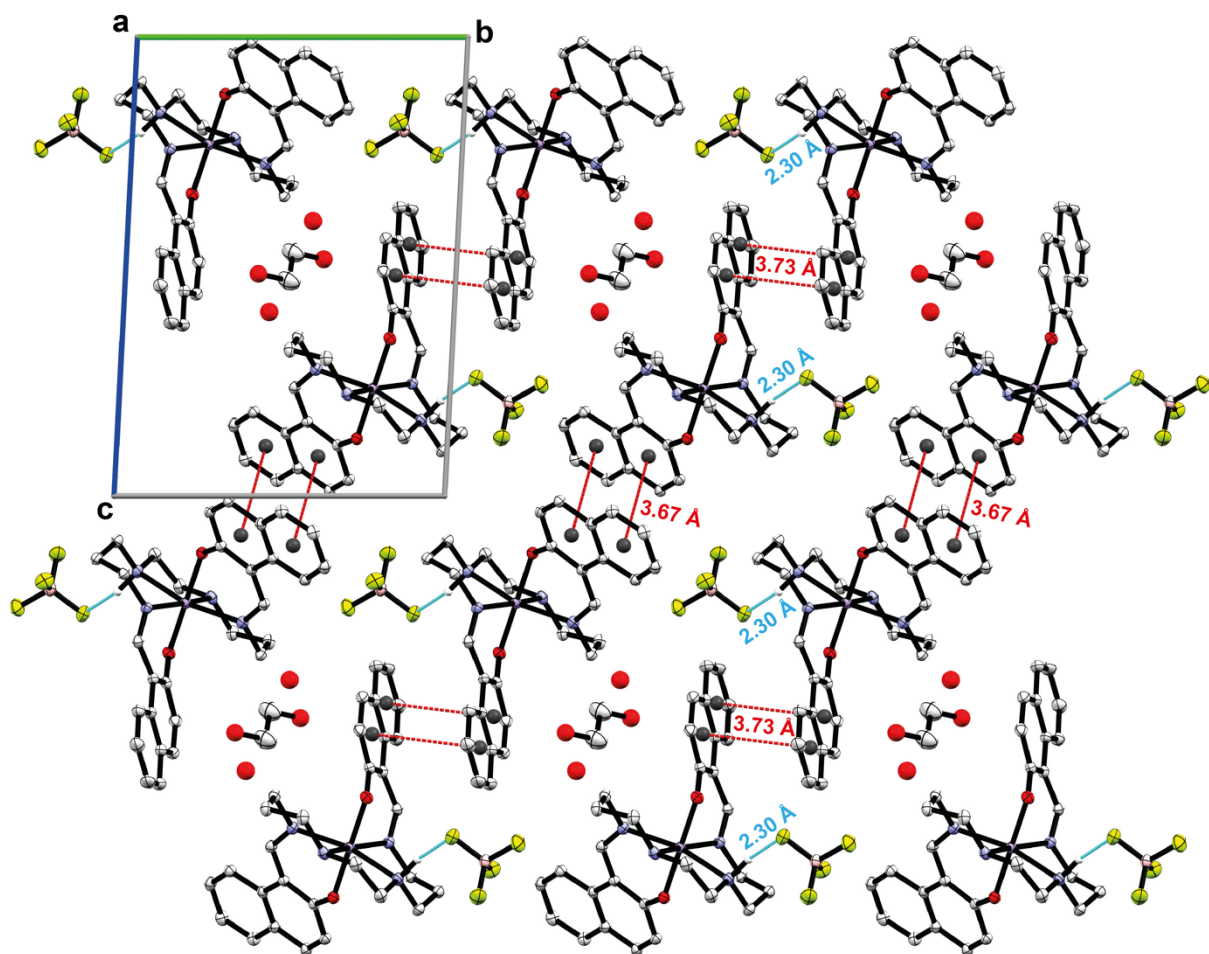


Figure S.10 Hydrogen bonding (**blue**) and π - π stacking (**red**) interactions in **3·0.5EtOH** with ellipsoids drawn at 50% atomic probability. Hydrogen atoms, except those involved in the hydrogen bonding, have been omitted for clarity.

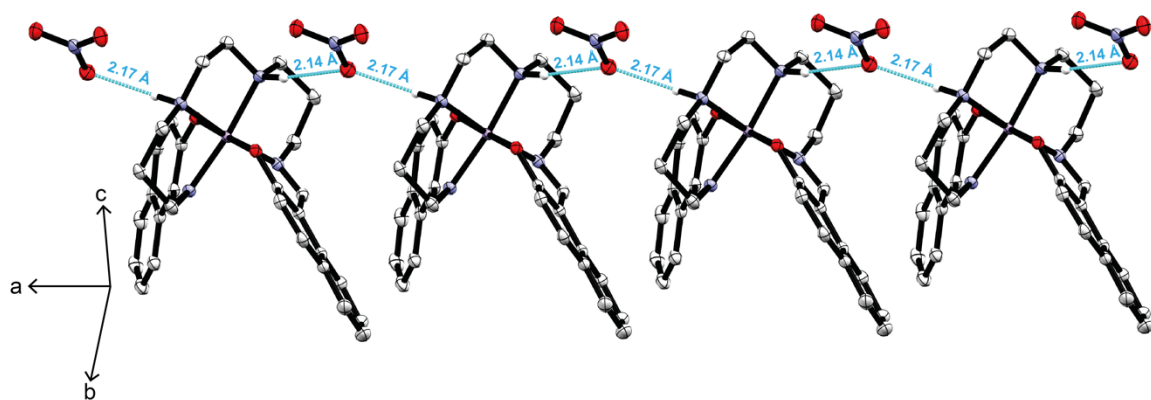


Figure S.11 1-D Hydrogen bonding network in **4** with ellipsoids drawn at 50% atomic probability. Hydrogen atoms, except those involved in the hydrogen bonding, have been omitted for clarity.

S.8 Infrared Spectra of 1, 2, 2·0.5EtOH, 3, 3·0.5EtOH and 4

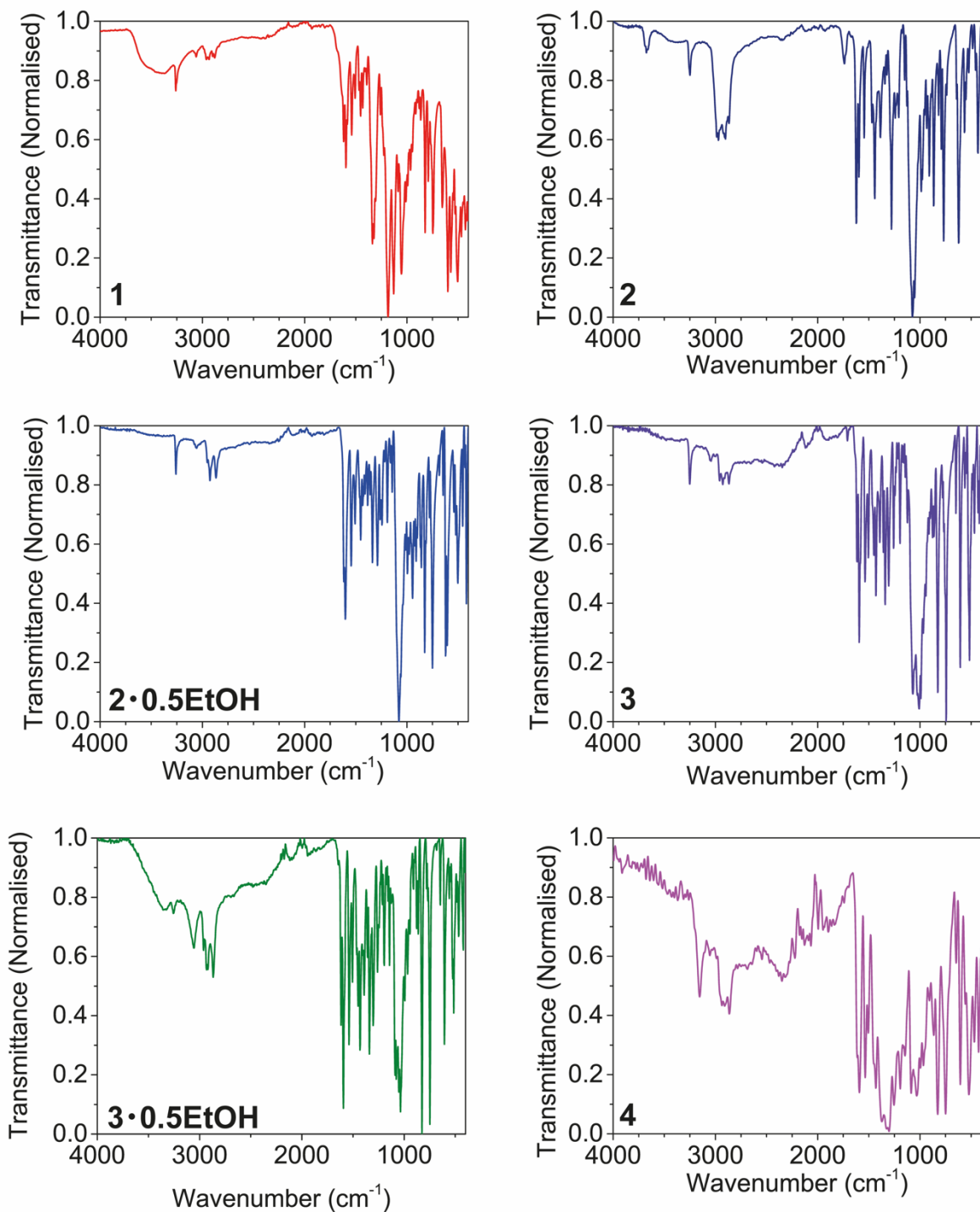


Figure S.12 Infrared spectra for complexes 1 – 4, 2·0.5EtOH and 3·0.5EtOH.

S.9 UV-Visible Spectra of **1** – **4**, **2**·0.5EtOH and **3**·0.5EtOH.

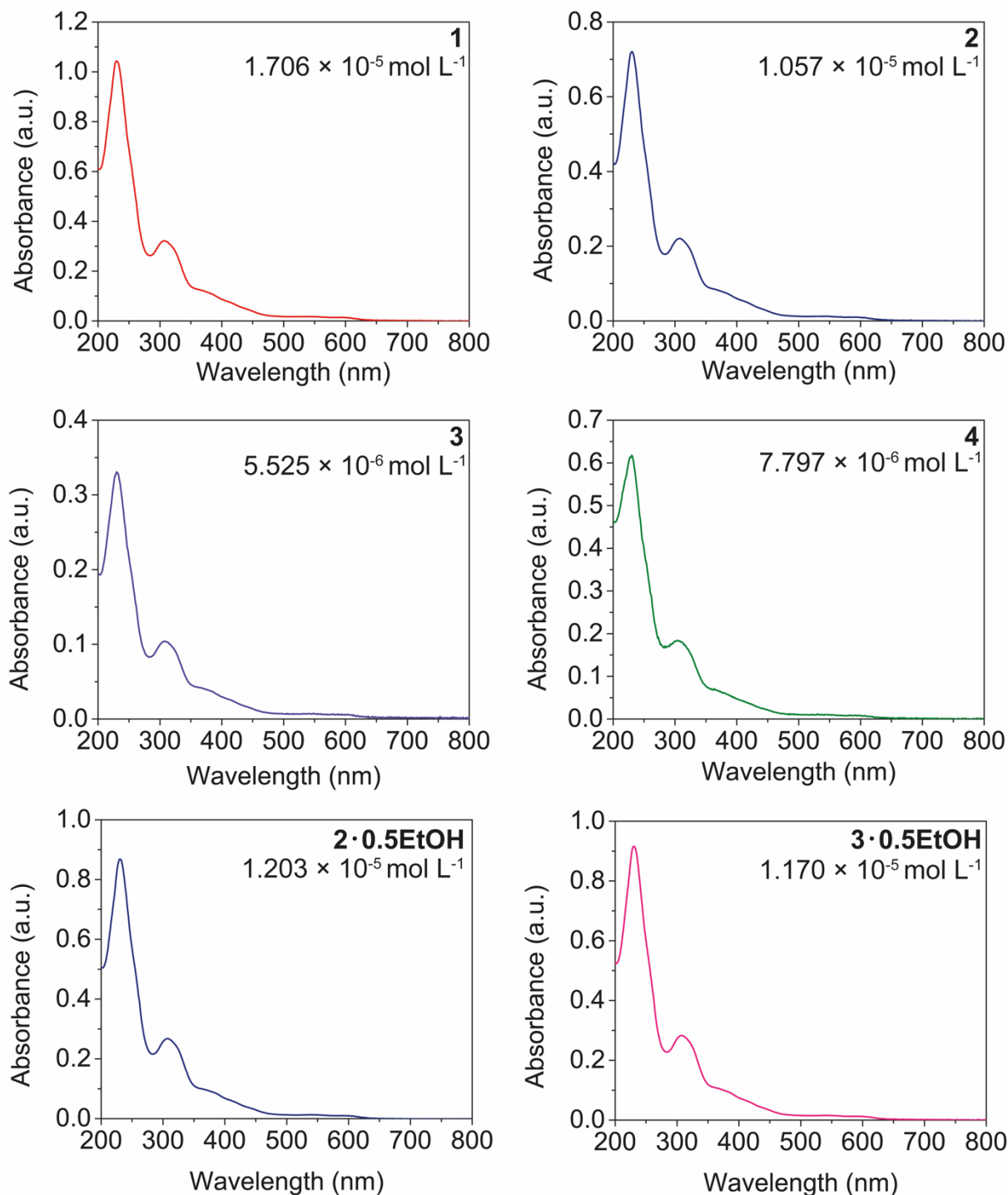


Figure S.13 UV-Visible spectra from 200 nm – 800 nm of **1** – **4**, **2**·0.5EtOH and **3**·0.5EtOH in acetonitrile with concentrations indicated on the spectra.

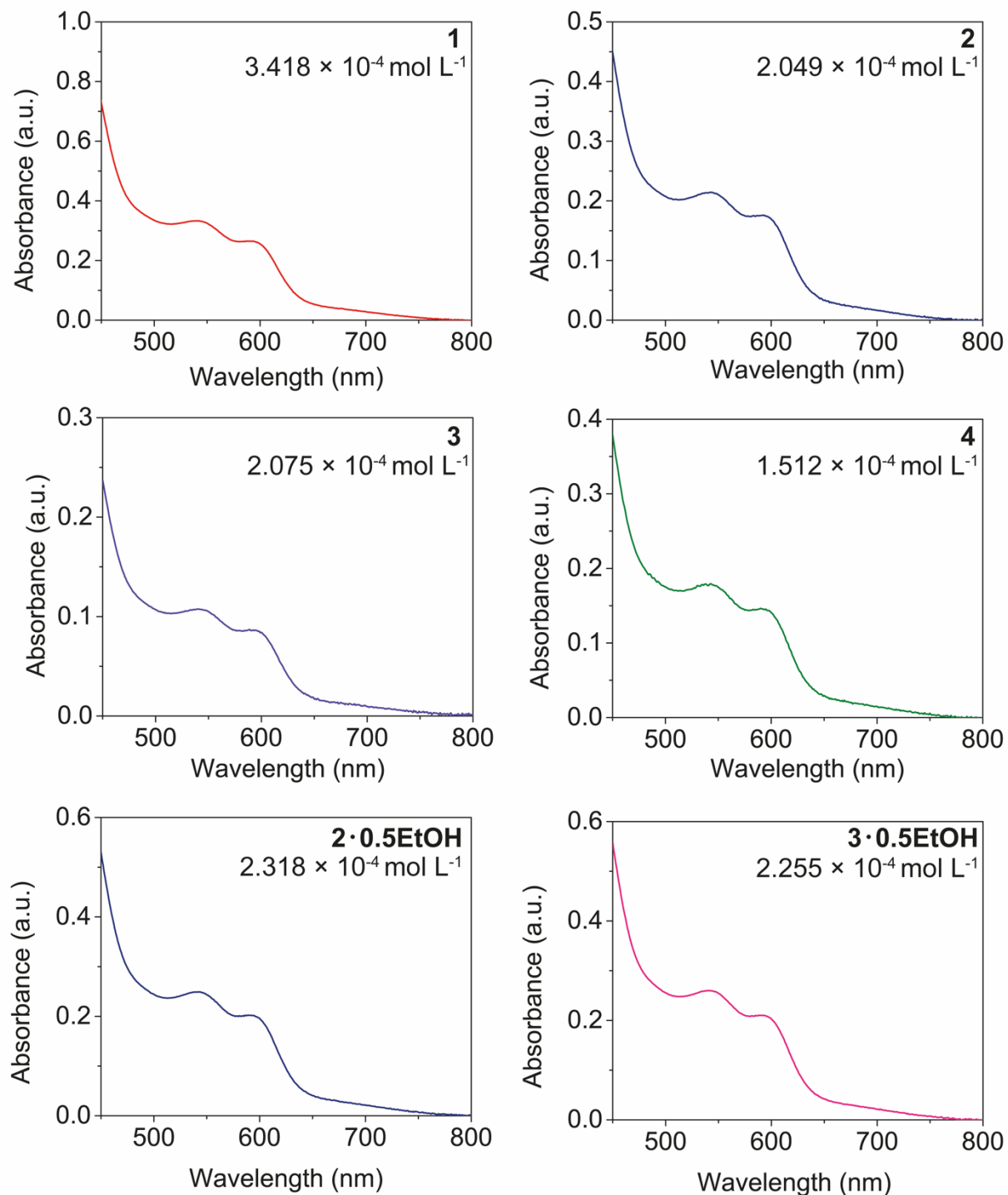


Figure S.14 UV-Visible spectra from 450 nm – 800 nm for **1 – 4**, **2·0.5EtOH** and **3·0.5EtOH** with concentrations indicated on the spectra.

S.10 Powder X-Ray Diffraction

Powder X-Ray diffraction (PXRD) experiments were carried out using a Bruker D2 Phaser with CuK α radiation $\lambda = 1.5418 \text{ \AA}$. Samples were used as is and measured on a zero-background silicon sample holder. The data was collected in the 2θ Range from $5 - 55^\circ$ in 0.01° increments at room temperature while rotating the sample at one rotation per minute in φ direction. Background due to fluorescence was subtracted. Normalised intensity plots of the experimental (top) and simulated (bottom) powder X-ray pattern of the compounds **1**, **2**, **3·0.5EtOH** and **4**.

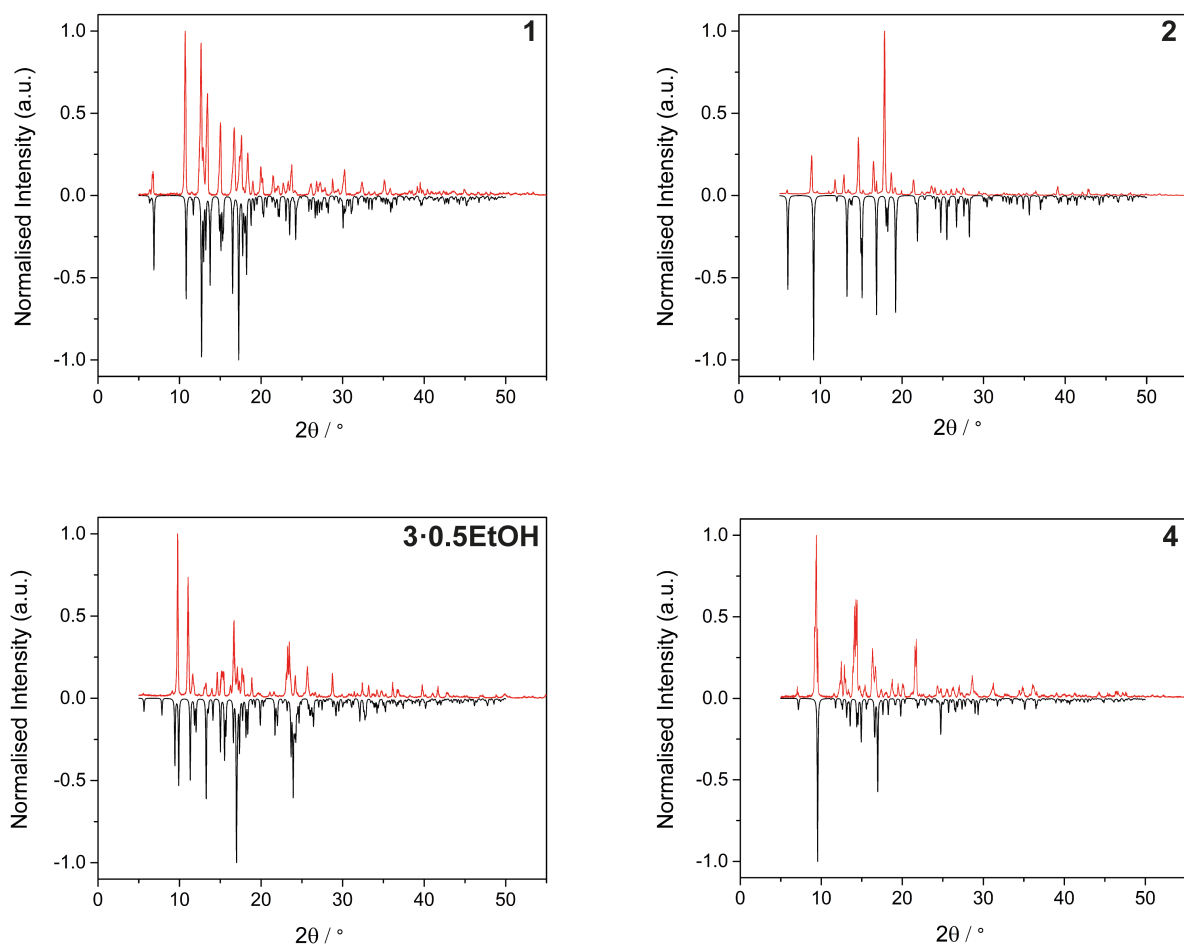


Figure S.15 PXRD pattern for **1**, **2**, **3·0.5EtOH** and **4**.

References

1. Stoll, S.; Schweiger, A. *J. Magn. Reson.* 2006, **178**, 42–55.
2. A. Hassan, L. Pardi, J. Krzystek, A. Sienkiewicz, P. Goy, M. Rohrer and L.-C. Brunel, *J. Magn. Reson.*, 2000, **142**, 300–312.
3. R. C. Clark and J. S. Reid, *Acta Crystallogr. Sect. A Found. Crystallogr.*, 1995, **51**, 887–897.
4. G. M. Sheldrick, *Acta Crystallogr. Sect. C Struct. Chem.*, 2015, **71**, 3–8.
5. M. Dommaschk, M. Peters, F. Gutzeit, C. Schütt, C. Näther, F. D. Sönnichsen, S. Tiwari, C. Riedel, S. Boretius and R. Herges, *J. Am. Chem. Soc.*, 2015, **137**, 7552–7555.
6. B. Gildea, M. M. Harris, L. C. Gavin, C. A. Murray, Y. Ortin, H. Müller-Bunz, C. J. Harding, Y. Lan, A. K. Powell and G. G. Morgan, *Inorg. Chem.*, 2014, **53**, 6022–6033.